Medical Image Analysis

Angshuman Paul

Assistant Professor

Department of Computer Science & Engineering

Microscopic Image Analysis

Types of Microscopic Medical Images

- Brightfield Microscopy
- Fluorescence Microscopy
- Phase Contrast Microscopy
- Quantitative Phase Microscopy

https://www.ncbi.nlm.nih.gov/books/NBK546149/

Brightfield Microscopy

- Density and thickness of a specimen are space-variant
- Specimen points absorb light differently
- The *condenser* plays the role of concentrating light coming from a light source at the specimen
- The specimen information is encoded in the intensity of light wave which reaches the objective
- Background or the part of the scene which does not contain dense objects tends to be bright in the resulting image

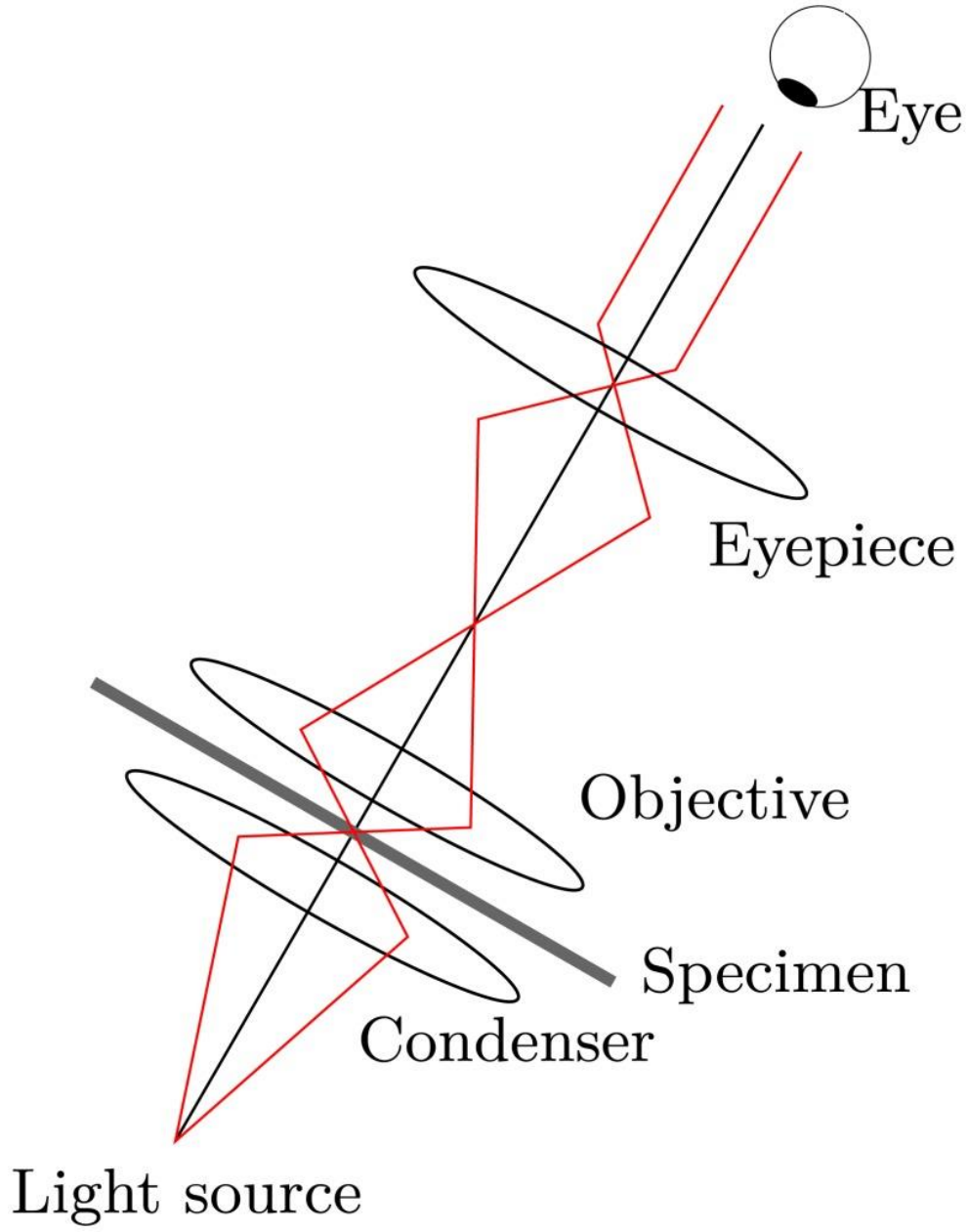

Brightfield Microscopy

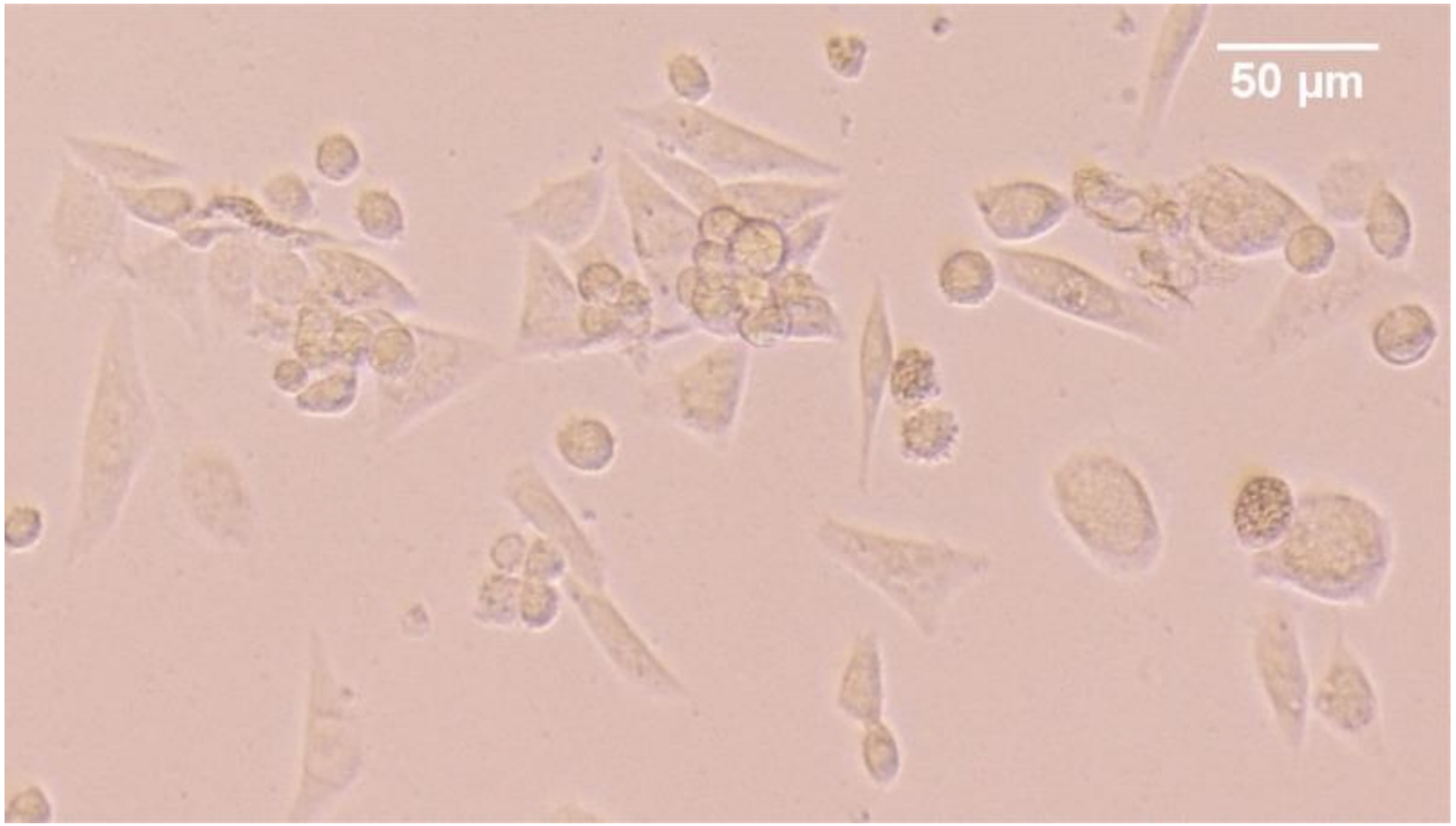

A microscopic image of a cell culture: The image was acquired using a Nikon Eclipse TE2000U microscope with a bright field objective of magnification 10× and NA = 0.3

Use of Stains for Histology and Cytology

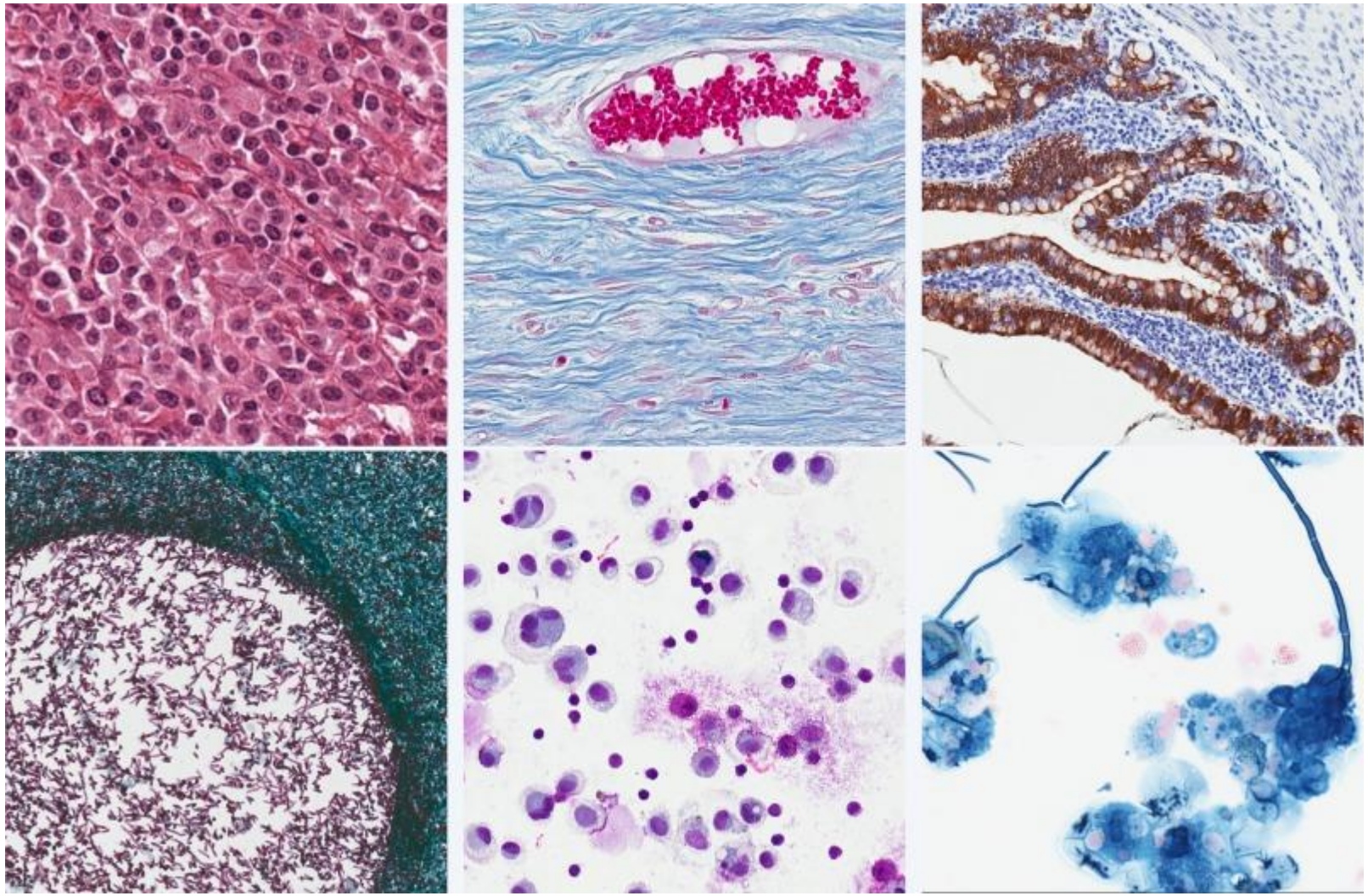

Top row: Hematoxylin-eosin, Azan, Multi-cytokeratin (AE1, AE3).
Bottom row: Grocott, May-Grünwald-Giemsa, Turnbull Blue. Images courtesy of FU Berlin, Germany.

Use of Stains for Histology and Cytology

- Highlights cellular structures
- Sections from tissue biopsies, cytology slides are often dyed or stained
- Most common form of stain in histology: mixture of hematoxylin and eosin
- Hematoxylin color stains cell nuclei blue
- Cytoplasm and other cellular structures are dyed in magenta by eosin
- Dyes are furthermore used to assess the amount of certain substances
  - e.g. copper or iron, or biologic structures adhering to certain biomarkers
- Besides a main color, often a secondary (or even third) color with strongly different spectral shape is used to dye other cellular compartments and enhance the contrast
  - The process is called counterstaining.

H&E Stain

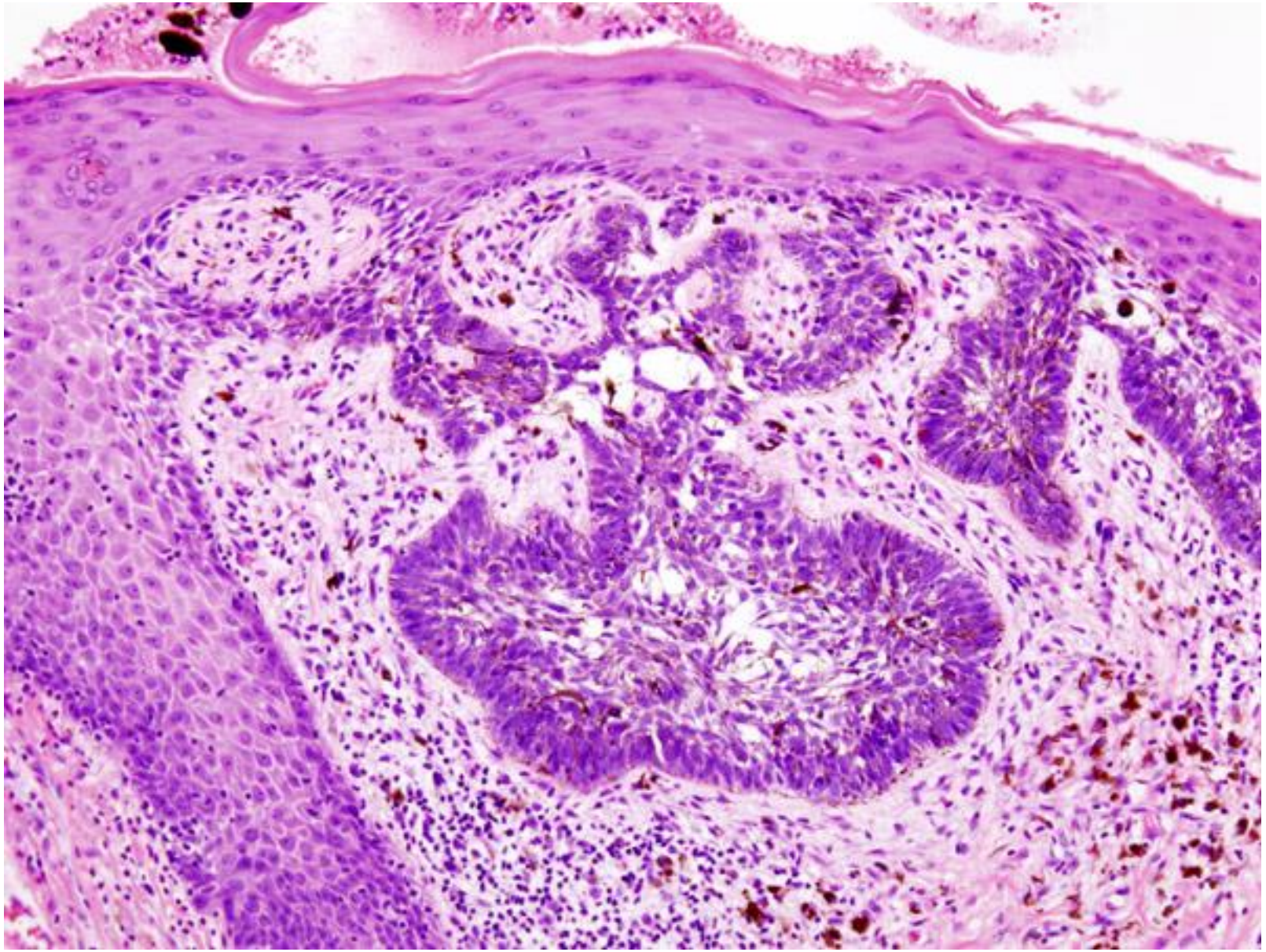

Normalization of H&E Stain

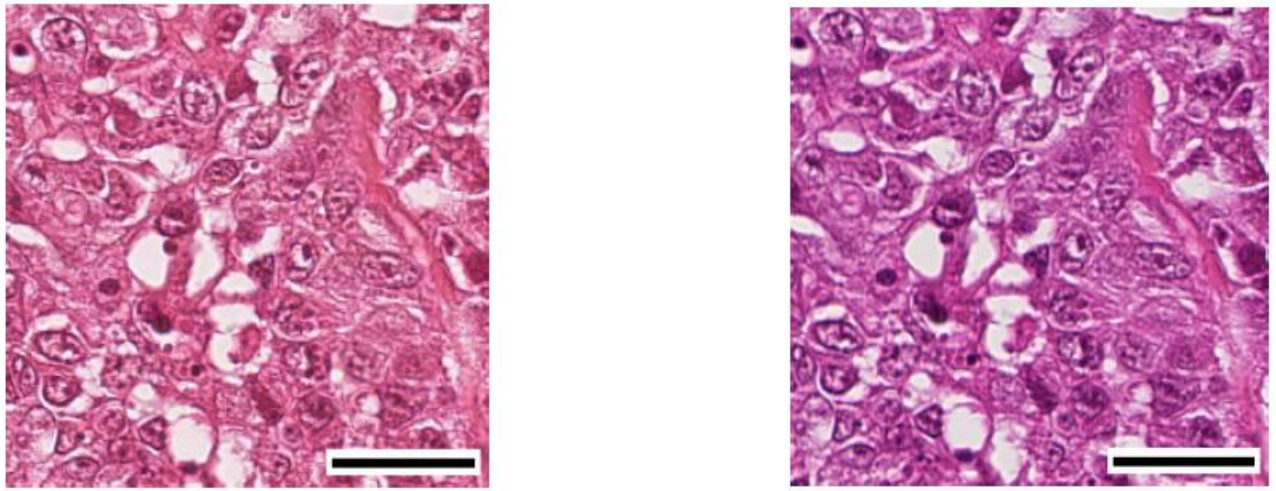

Figure 1. (**a**) Image acquired using Aperio Scanscope XT scanner. (**b**) Image acquired using Hamamatsu Nanozoomer 2.0-HT scanner. Scale bar, 16.95 µm.

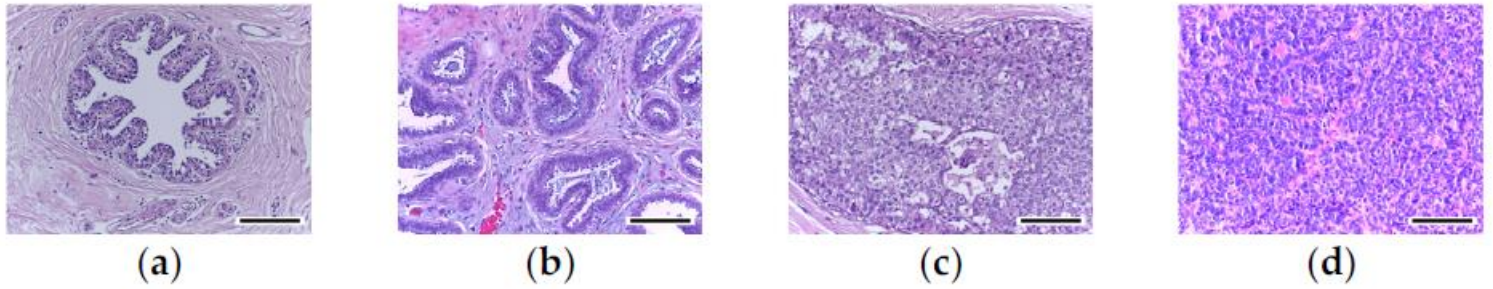

Figure 2. Microscopy images labeled with the predominant cancer type in each image: (**a**) Normal, (**b**) benign, (**c**) in situ carcinoma, and (**d**) invasive carcinoma. Scale bar, 164 µm.

https://www.ncbi.nlm.nih.gov/pmc/articles/PMC10452714/

Normalization of H&E Stain

- Visual inconsistencies due to variations of staining due to
  - Staining protocols
  - Slide preparation techniques
  - Imaging conditions
- Change in the distribution of data
- Performance degradation in the downstream tasks
- Stain normalization: standardization of appearance

Normalization of H&E Stain

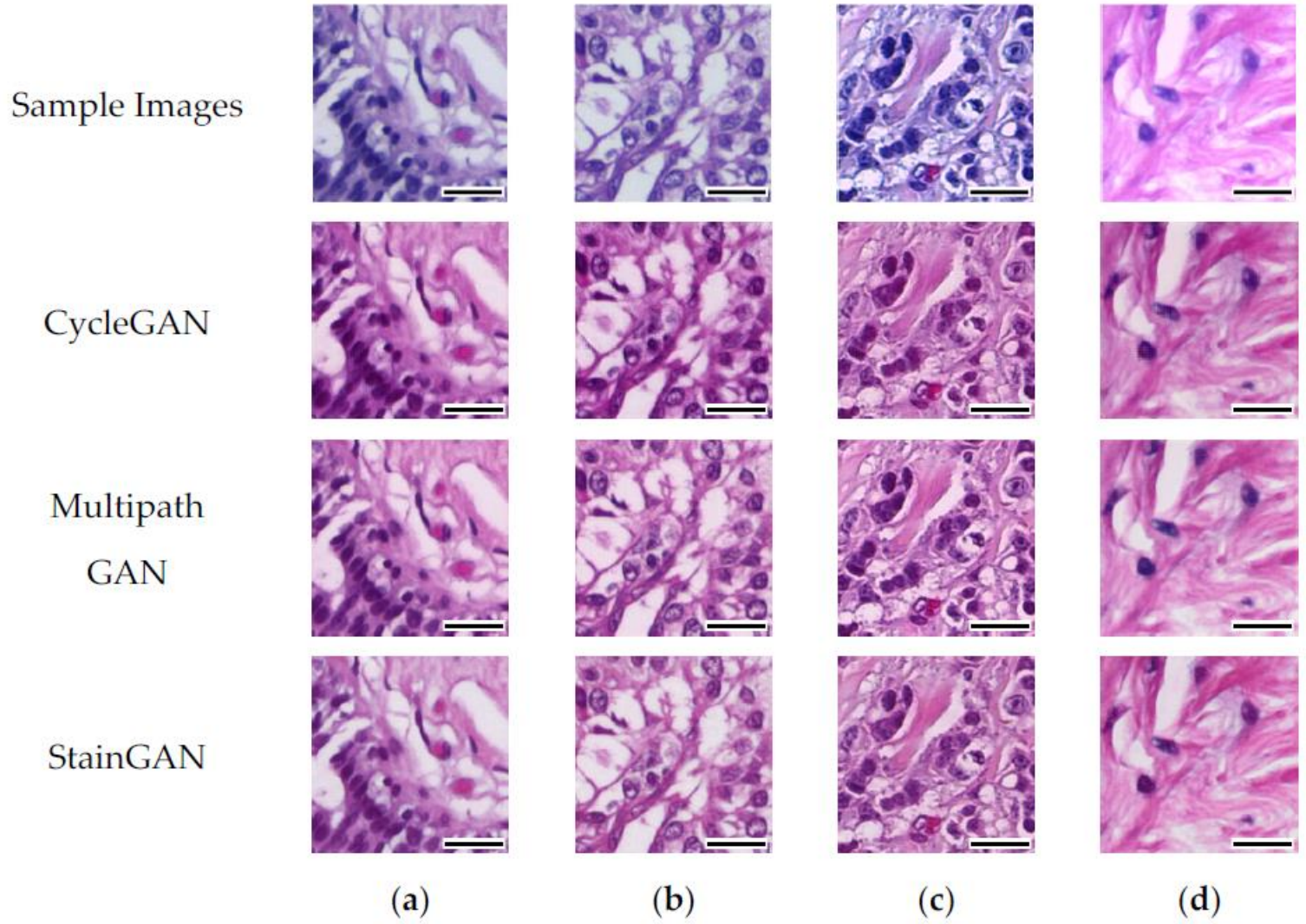

Figure 3. CycleGAN, MultipathGAN, and StainGAN normalized sample images from the dataset, labeled with the predominant cancer type in each image. (**a**) Benign, (**b**) in situ carcinoma, (**c**) invasive carcinoma, and (**d**) normal. Scale bar, 31.5 µm.

https://www.ncbi.nlm.nih.gov/pmc/articles/PMC10452714/

CycleGAN for Normalization of H&E Stain

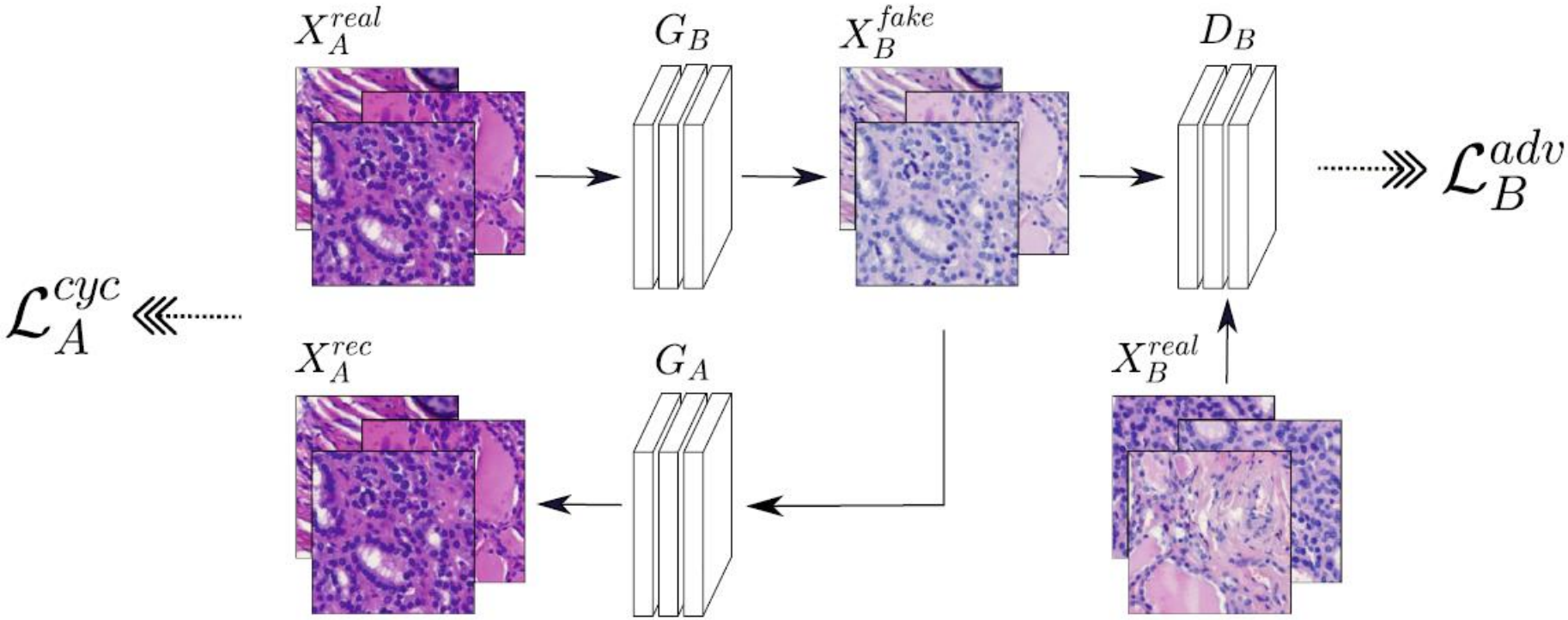

Fig. 1 Illustration of the applied CycleGAN architecture for mapping images from domain *A* to domain *B*. A real sample image X_A^{real} is mapped to domain *B* by the generator $G_B : X_A^{real} \rightarrow X_B^{fake}$ and then back to domain *A* by the generator $G_A : X_B^{fake} \rightarrow X_A^{rec}$. The discriminator D_B differentiates between the generated image X_B^{fake} and a real sample image X_B^{real}. The same process is done for the reverse direction when mapping a real sample image X_B^{real} from domain *B* to domain *A* and backwards, i.e $X_B \xrightarrow{G_A} X_A^{fake} \xrightarrow{G_B} X_B^{rec}$. During training, the loss is computed by the adversarial loss $\mathcal{L}^{adv}$ and the cycle consistency loss $\mathcal{L}^{cyc}$

Normalization of HE-stained histological images using cycle consistent generative adversarial networks

Fluorescence Microscopy

- Some special materials, when illuminated with light having a specific wavelength, emit light with another wavelength
- An excitation filter is required to select a part of the electromagnetic spectrum for exciting the fluorescent materials in specimen
- Another filter is then utilized to separate the emitted light from that used in the excitation process

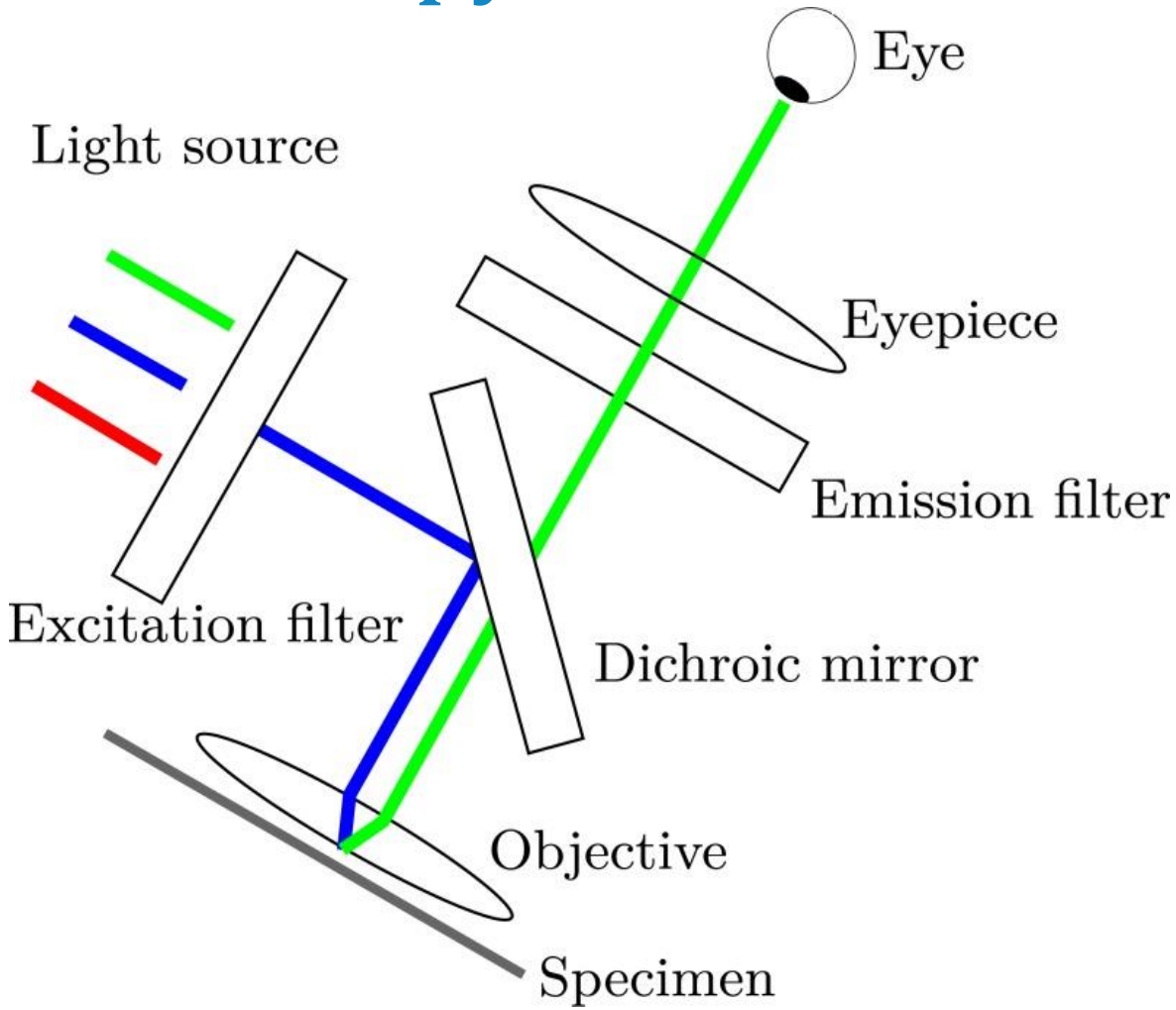

Fluorescence Microscopy

- Fluorescence microscopes deliver images of high contrast when compared to bright field images
- Fluorescence can be incited by specific biological or physical processes
- Firstly, staining may cause some undesired effects on the sample under study
- Usually does not revel structural information

Fluorescence Microscopy

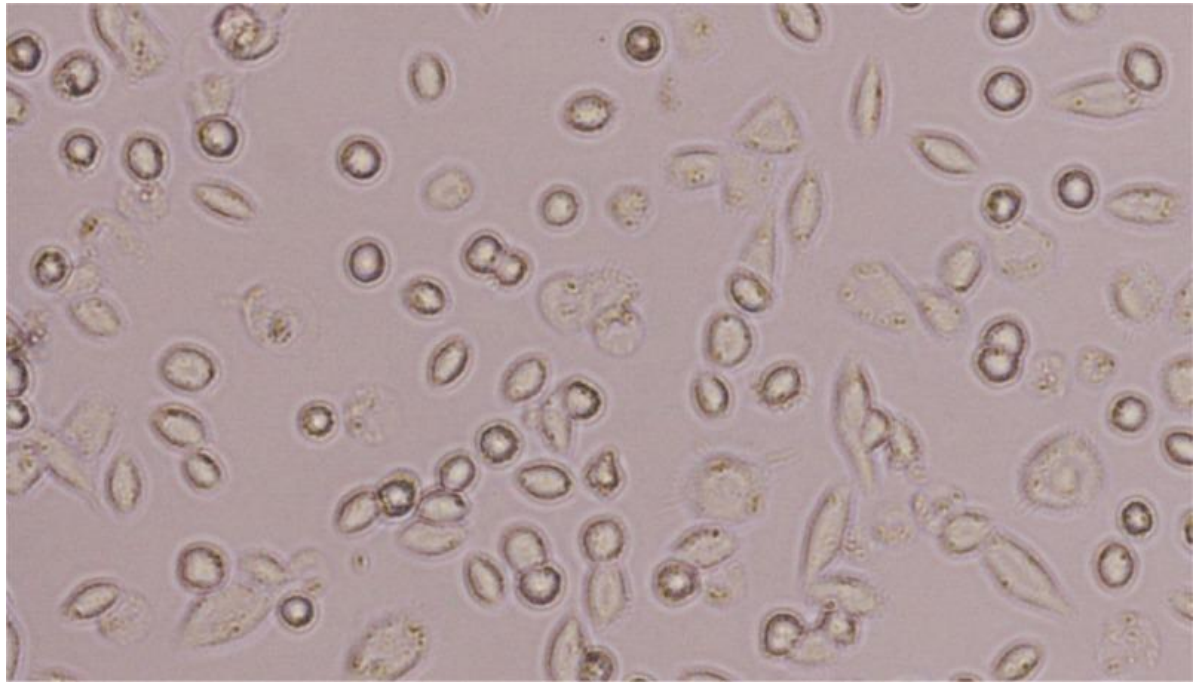

A bright field image of Chinese hamster ovary (CHO) cells

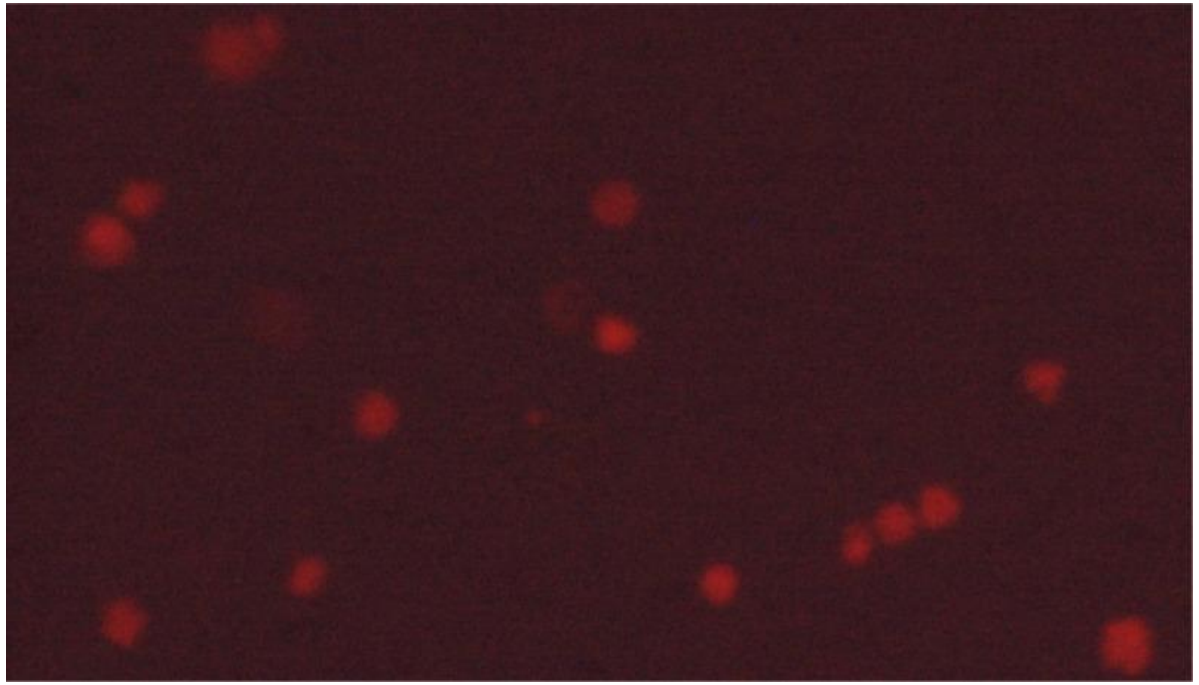

The same scene at the left-hand side but seen under a fluorescent channel. Red spots indicate dead cells

Mitosis Detection for Breast Cancer Grading

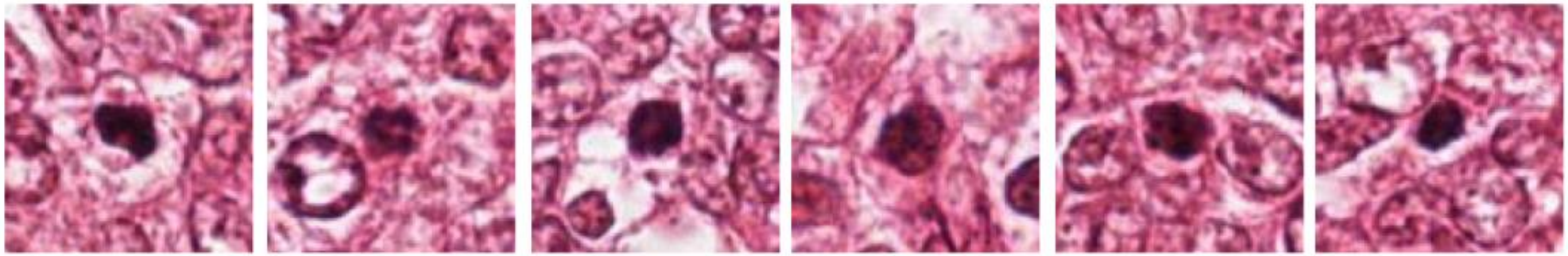

Fig. 1 An illustration of the visual similarity between true mitotic processes and confounding false positives. (a)–(c) True mitoses. (d)–(f) Confounding nonmitotic figures.

Mitosis Detection for Breast Cancer Grading

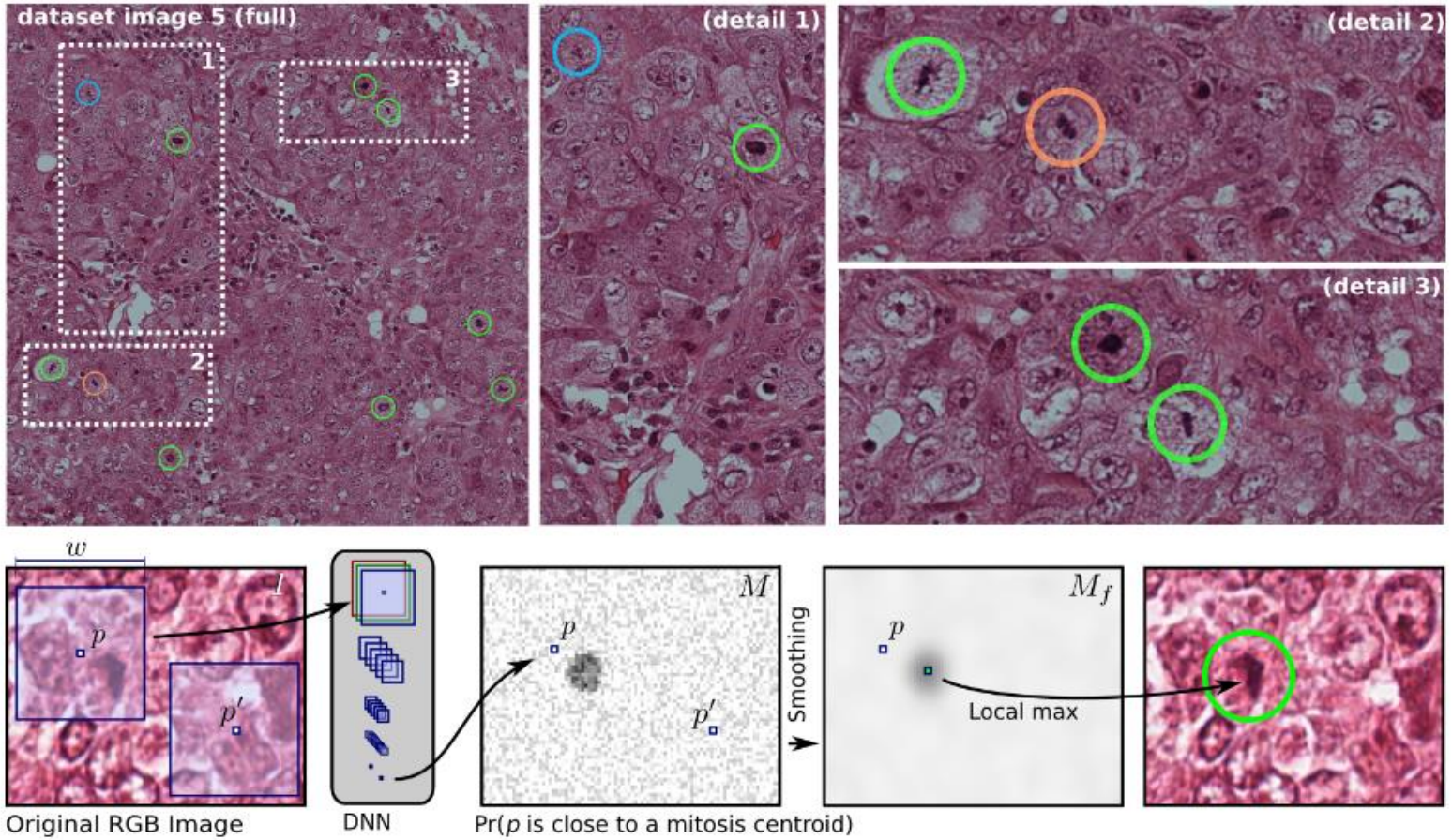

Fig. 1. *Top left:* one image (4 MPixels) corresponding to one of the 50 high power fields represented in the dataset. Our detected mitosis are circled green (true positives) and red (false positives); cyan denotes mitosis not detected by our approach. *Top right:* details of three areas (full-size results on the whole dataset in supplementary material). Note the challenging appearance of mitotic nuclei and other very similar non-mitotic structures. *Bottom:* overview of our detection approach.

https://people.idsia.ch/~juergen/miccai2013.pdf

Mitosis Detection for Breast Cancer Grading

$$BR = \frac{100 * B}{1+R+G} \times \frac{256}{1+B+R+G}$$

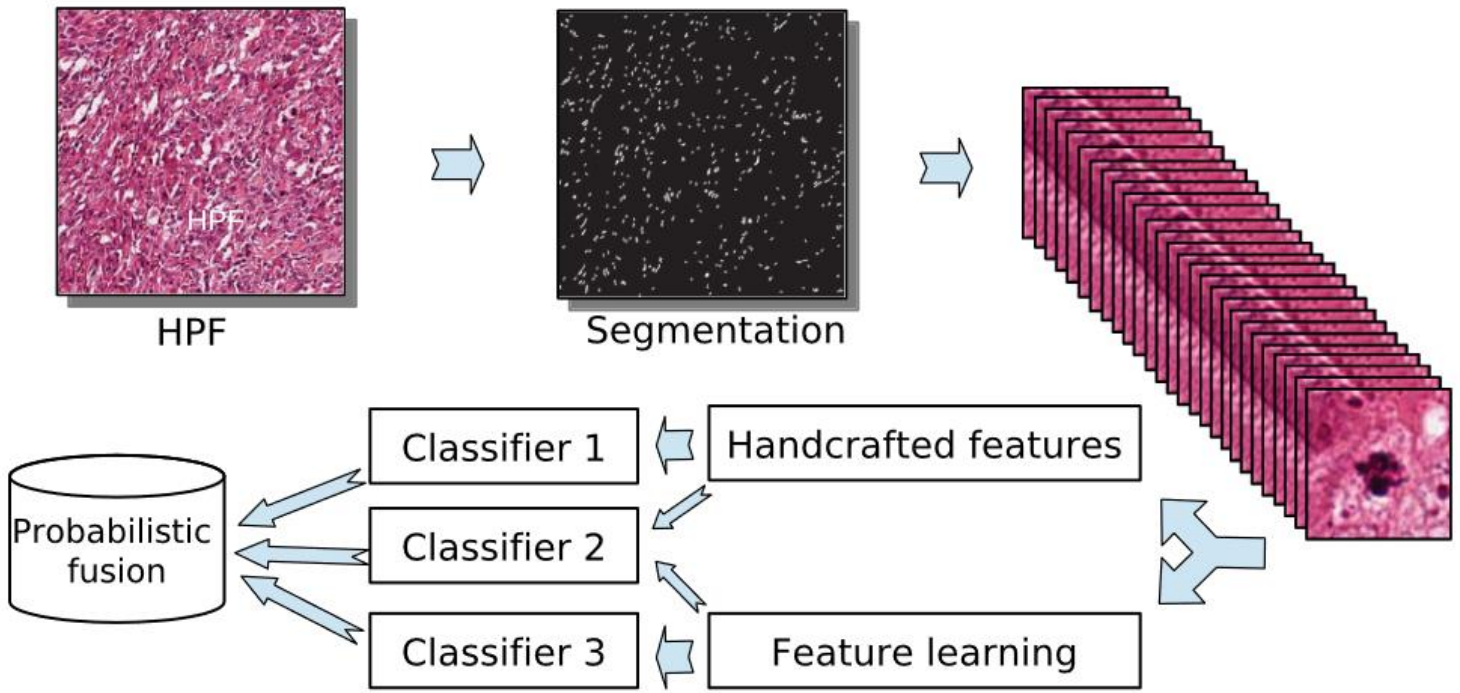

Fig. 2 Workflow of our methodology. Blue-ratio thresholding[15] is first applied to segment mitosis candidates. On each segmented blob, handcrafted features are extracted and classified via a random forests classifier. Meanwhile, on each segmented 80×80 patch, convolutional neural networks (CNN)[11] are trained with a fully connected regression model as part of the classification layer. For those candidates that are difficult to classify (ambiguous result from the CNN), we train a second-stage random forests classifier on the basis of combining CNN-derived and handcrafted features. Final decision is obtained via a consensus of the predictions of the three classifiers.

https://www.ncbi.nlm.nih.gov/pmc/articles/PMC4479031/pdf/JMI-001-034003.pdf

Mitosis Detection for Breast Cancer Grading

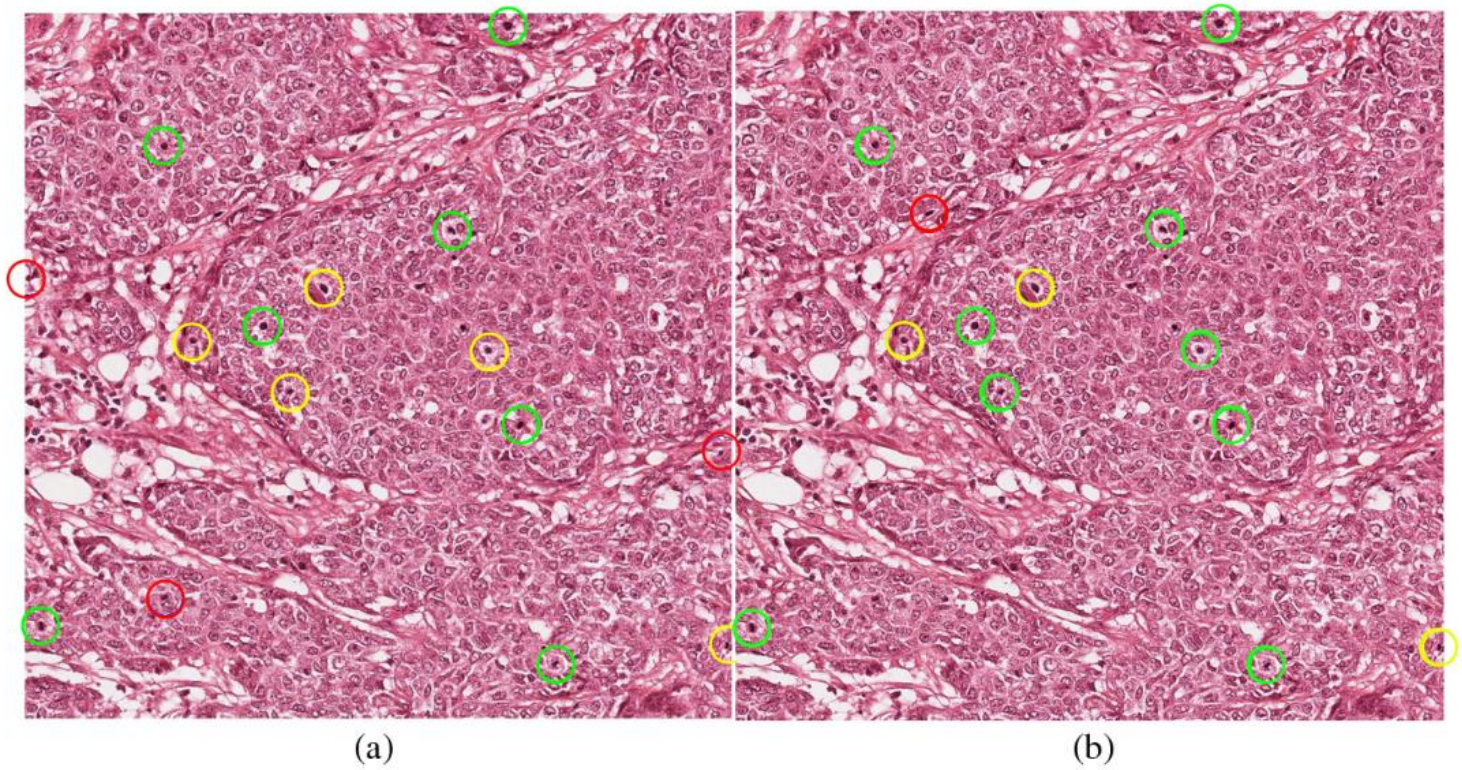

Fig. 9 Mitoses identified by CNN and HC + CNN as TP (green circles), FN (yellow circles), and FP (red circles) on a HPF of ICPR12 dataset. (a) Only using CNN leads to 7 TPs, 5 FNs and 3 FPs. (b) Using HC and CNN leads to 9 TPs, 3 FNs and 1 FP, which clearly outperforms the use of CNN alone.

Thyroid Cancer Diagnosis

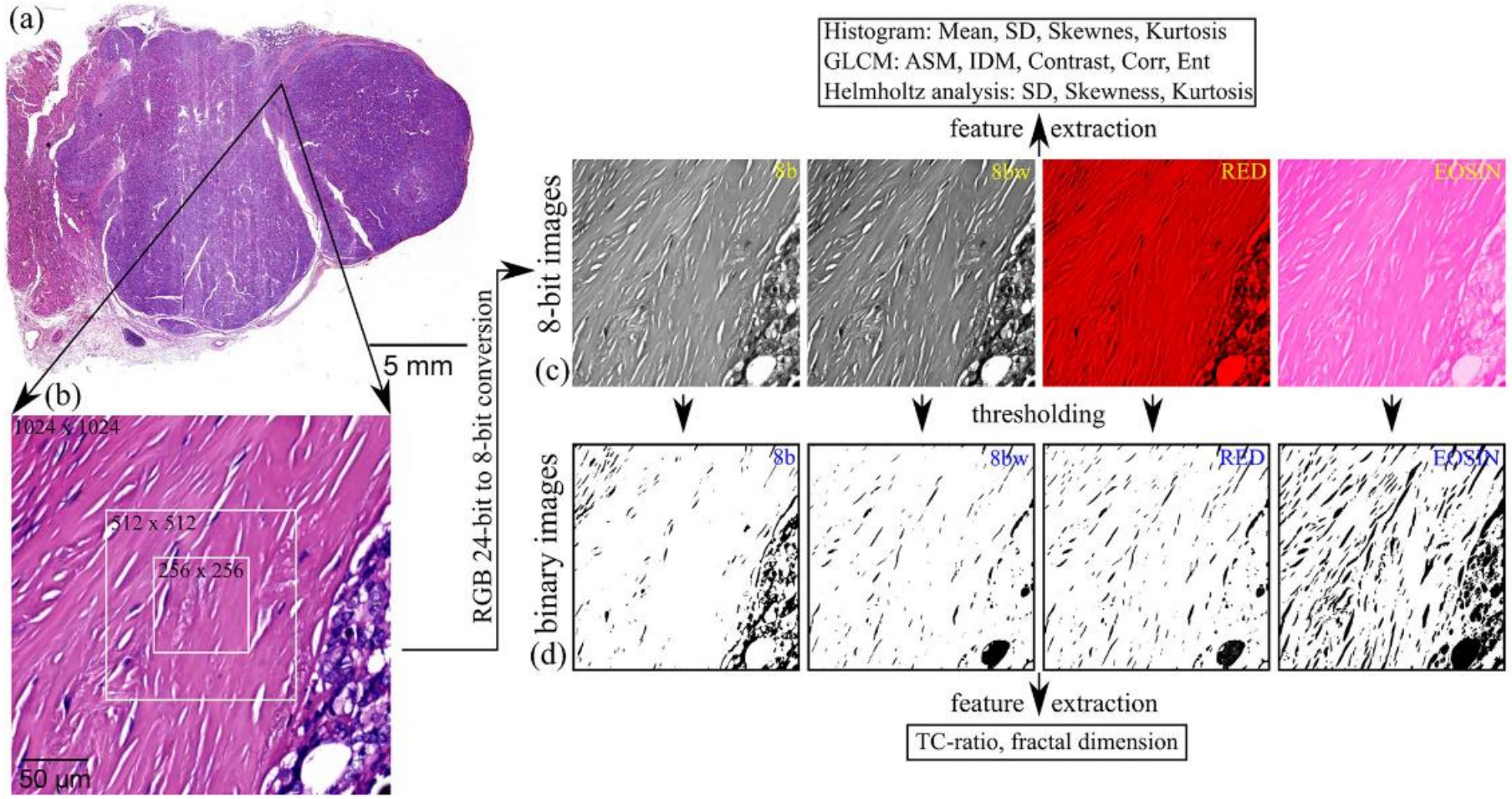

Figure 1. The feature extraction workflow: (**a**) whole slide image acquisition; (**b**) cropping of image tiles with different sizes (i.e., 1024×1024, 512×512, 256×256) within nodule capsules areas; (**c**) RGB to 8-bit conversion using four strategies (i.e., 8b, 8bw, RED, EOSIN) and subsequent feature extraction using the histogram, GLCM and Helmholtz analysis; (**d**) binarization of 8-bit images and subsequent feature extraction (i.e., TC-ratio, fractal dimension).

Thyroid Cancer Diagnosis

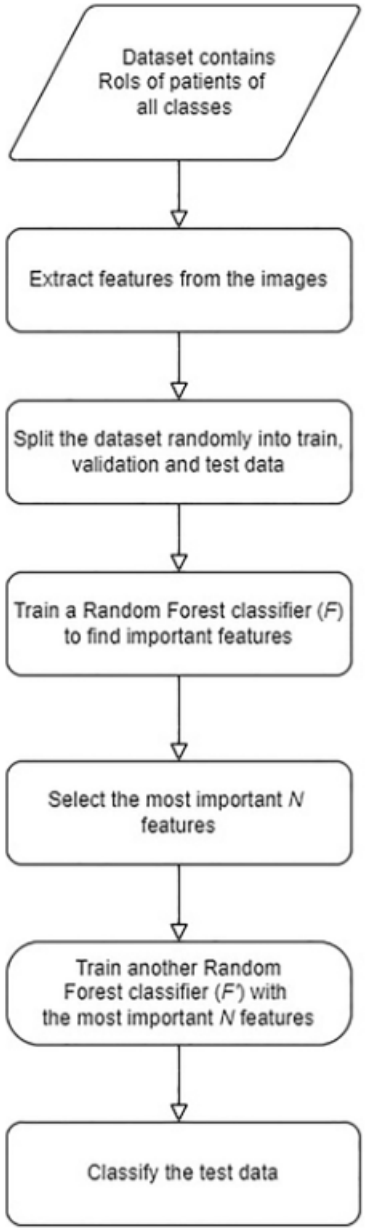

Figure 2. Flowchart showing the experimental steps of the proposed method.

Gland Segmentation In histopathology Images

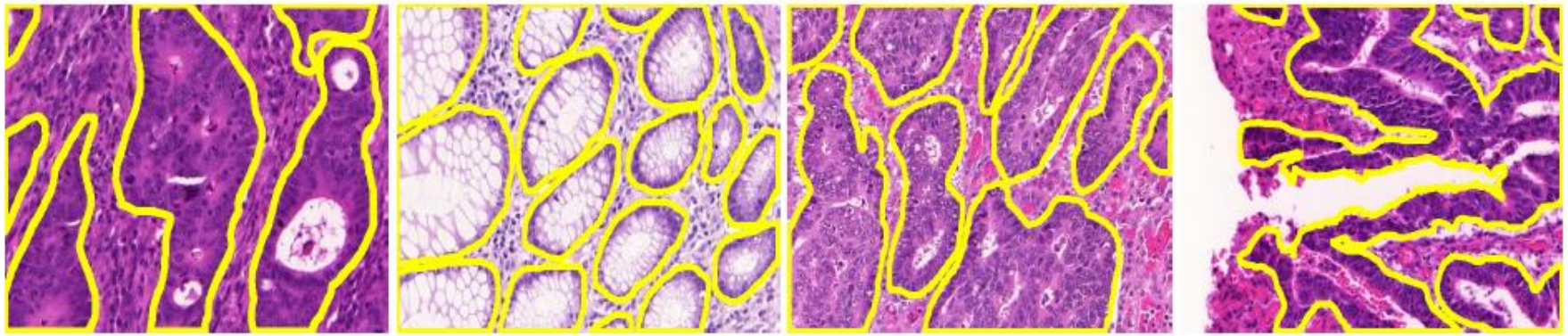

Figure 1: Sample histology images (Sirinukunwattana et al., 2017) with variations in color, contrast and gland structures. Gland boundaries are shown in yellow and the region inside the gland boundaries denotes the glands: (a) low contrast image, (b) well-shaped glands, (c) glands with touching boundaries, and (d) highly deformed glands.

Gland Segmentation In histopathology Images

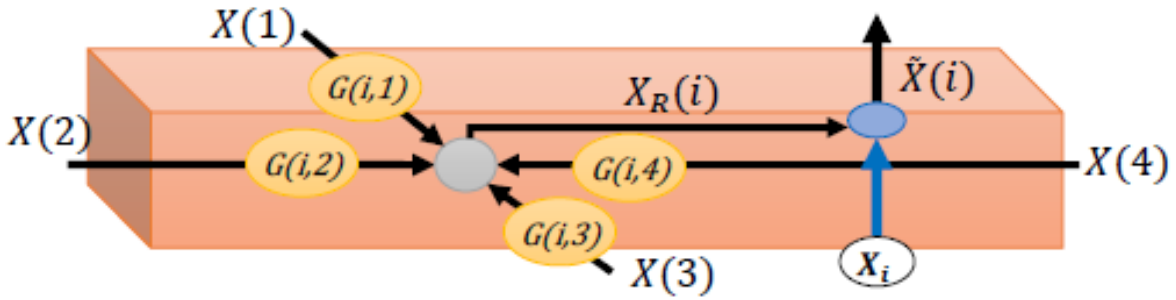

Figure 2: The Gated Feature Interaction (GFI) block (with four neighbors as an example): $X(1)$ to $X(4)$ are the input feature vectors from the neighbors coming through gates $G(i,\cdot)$. The input feature vector, and the resultant feature vector for pixel i are $\mathbf{X}_i$, and $\mathbf{X}_R(i)$ respectively.

Gland Segmentation In histopathology Images

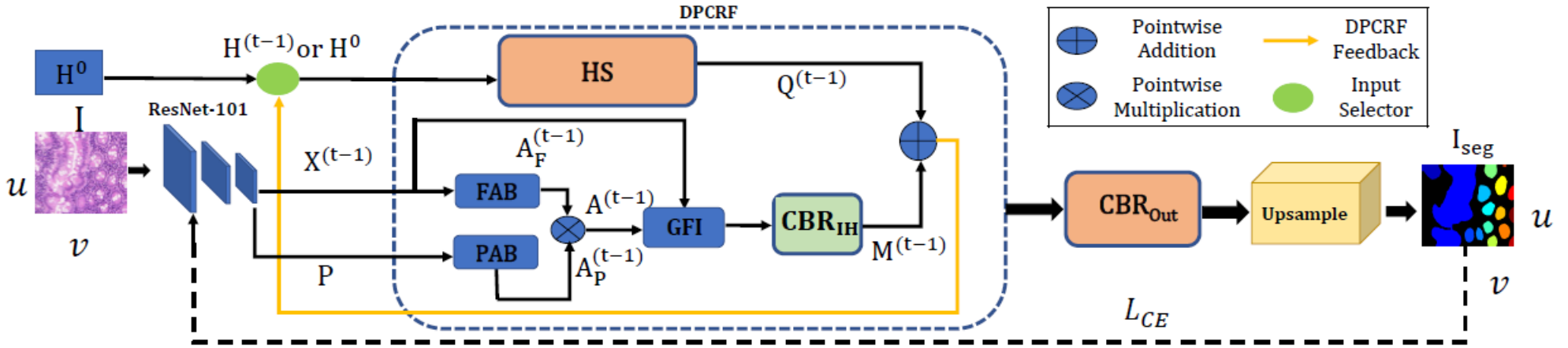

Figure 3: The block diagram of the proposed method. ResNet-101 generates a convolution map $\mathbf{X}^{(t-1)}$ for an input image $\mathbf{I}$. $\mathbf{X}^{(t-1)}$ is processed parallelly by a feature adjacency block (FAB) and a positional adjacency block (PAB) to generate an adjacency matrix $\mathbf{A}^{(t-1)}$. Subsequently a gated feature interaction block (GFI) uses $\mathbf{A}^{(t-1)}$ and $\mathbf{X}^{(t-1)}$ to generate an intermediate convolution map. This convolution map is subsequently processed by CBR_{IH} to produce $\mathbf{M}^{(t-1)}$. Similarly, either an initial hidden state $\mathbf{H}^0$ (at the first iteration) or $\mathbf{H}^{(t-1)}$ (at all other iterations) is processed through the HS block to generate a convolutional map $\mathbf{Q}^{(t-1)}$. Afterwards $\mathbf{Q}^{(t-1)}$ is added with $\mathbf{M}^{(t-1)}$ to produce $\mathbf{H}^t$ for the next iteration. After T iterations in DPCRF, the final hidden state $\mathbf{H}^T$ is passed through CBR_{Out} and subsequently upsampled to generate segmentation map I_{seg} at the output.

Gland Segmentation In histopathology Images

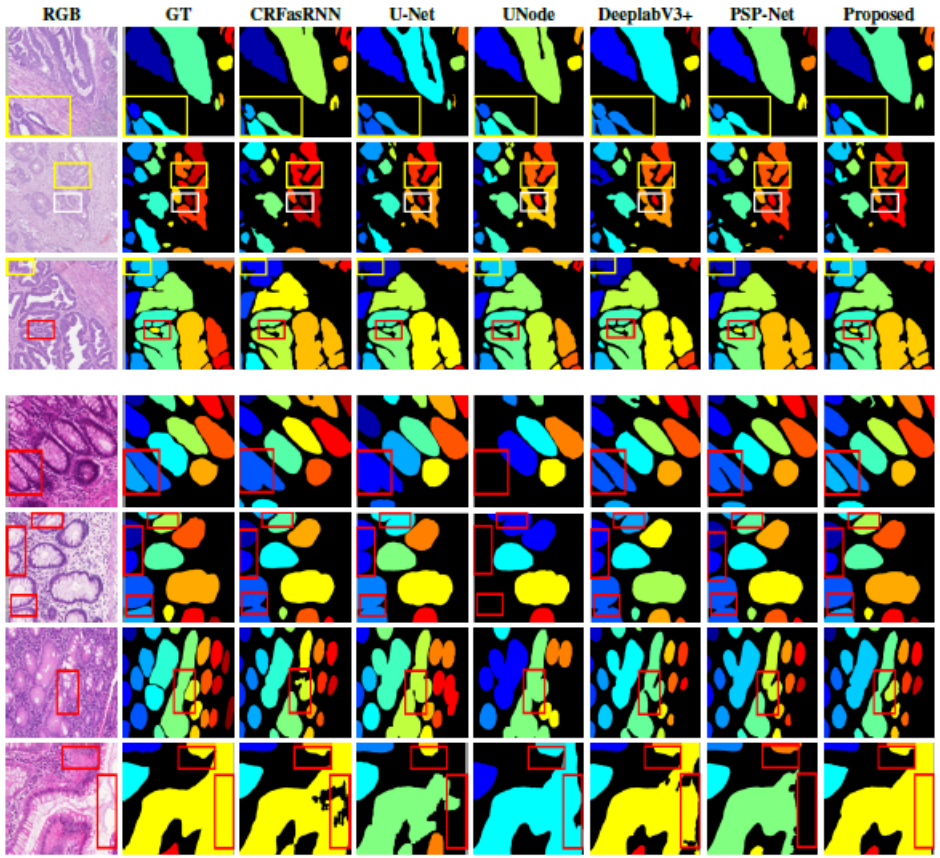

Figure 4: Segmentation results showing the performance of different methods (in different columns) on example images of CRAG dataset (rows 1-3) and GlaS dataset (rows 4-7).

Gland Segmentation In histopathology Images

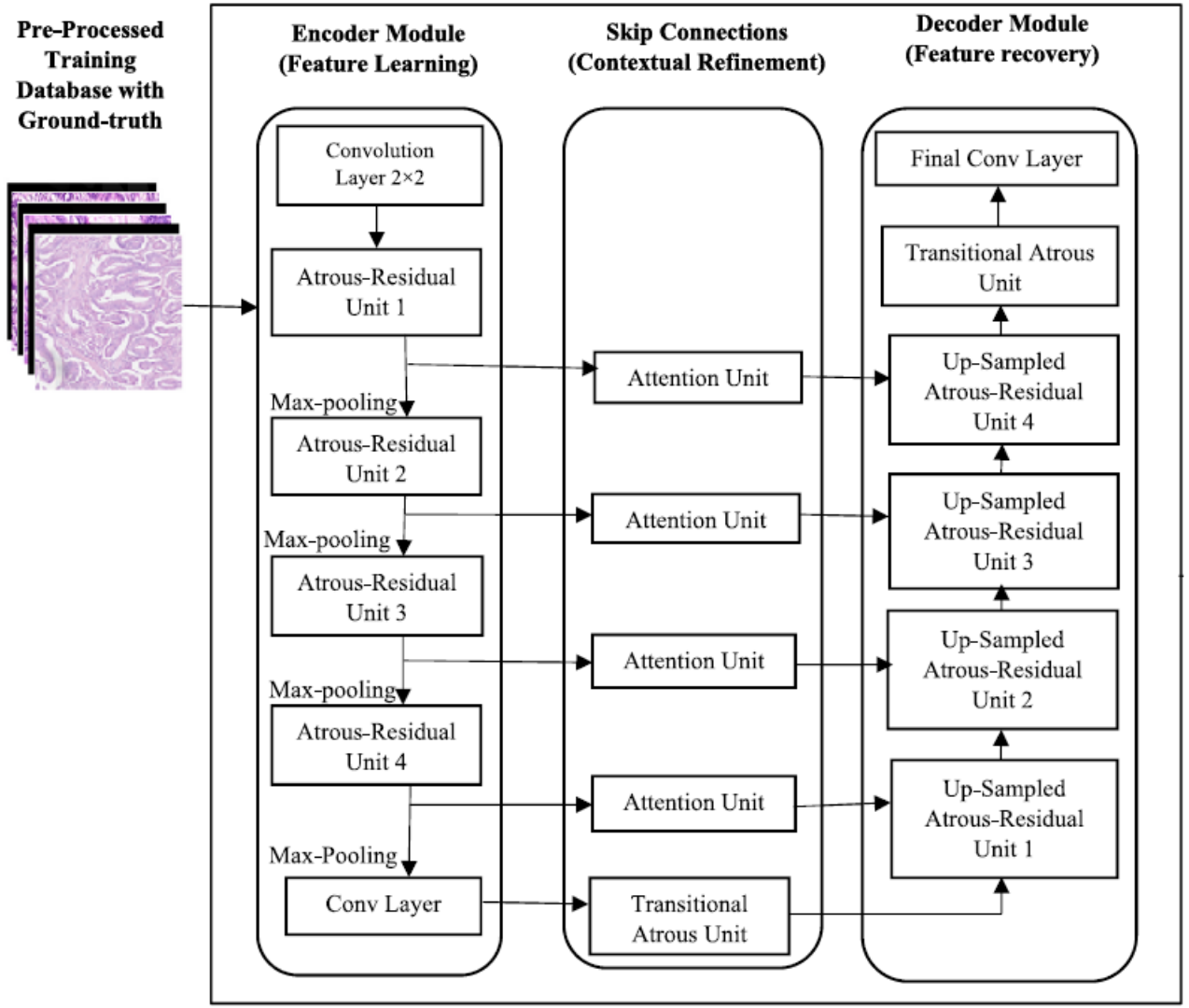

Classification Performance Measures

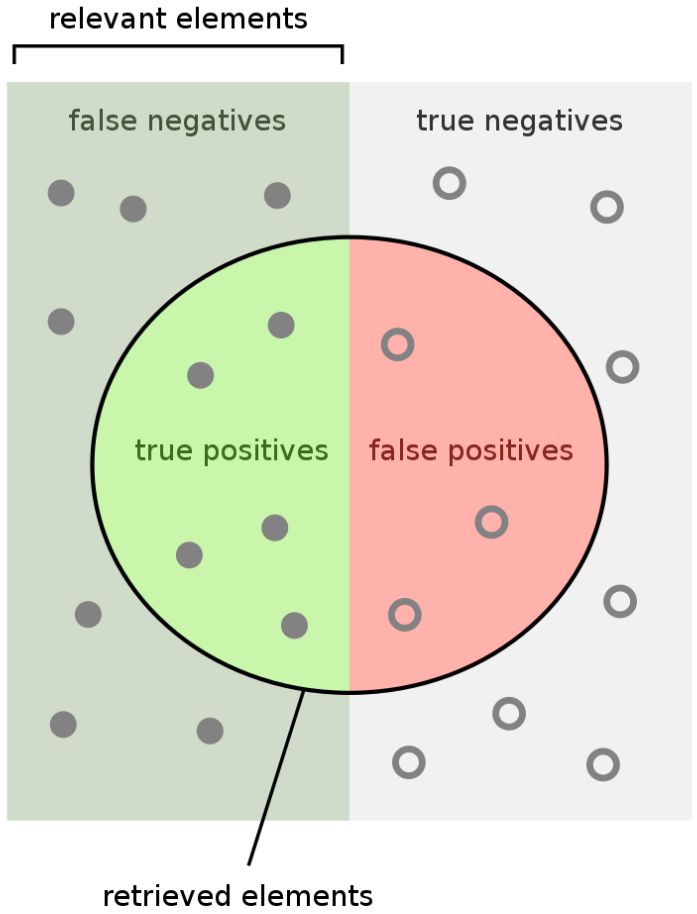

$$F_1 = \frac{2 * Re * Pr}{Re + Pr}$$

How many retrieved items are relevant?

Precision = $\frac{\text{green}}{\text{green + red}}$

How many relevant items are retrieved?

Recall = $\frac{\text{green}}{\text{green + dark green}}$

Area Under ROC Curve

$$\text{TPR /Recall / Sensitivity} = \frac{TP}{TP + FN}$$

$$\text{Specificity} = \frac{TN}{TN + FP}$$

$$\text{FPR} = 1 - \text{Specificity}$$

$$= \frac{FP}{TN + FP}$$

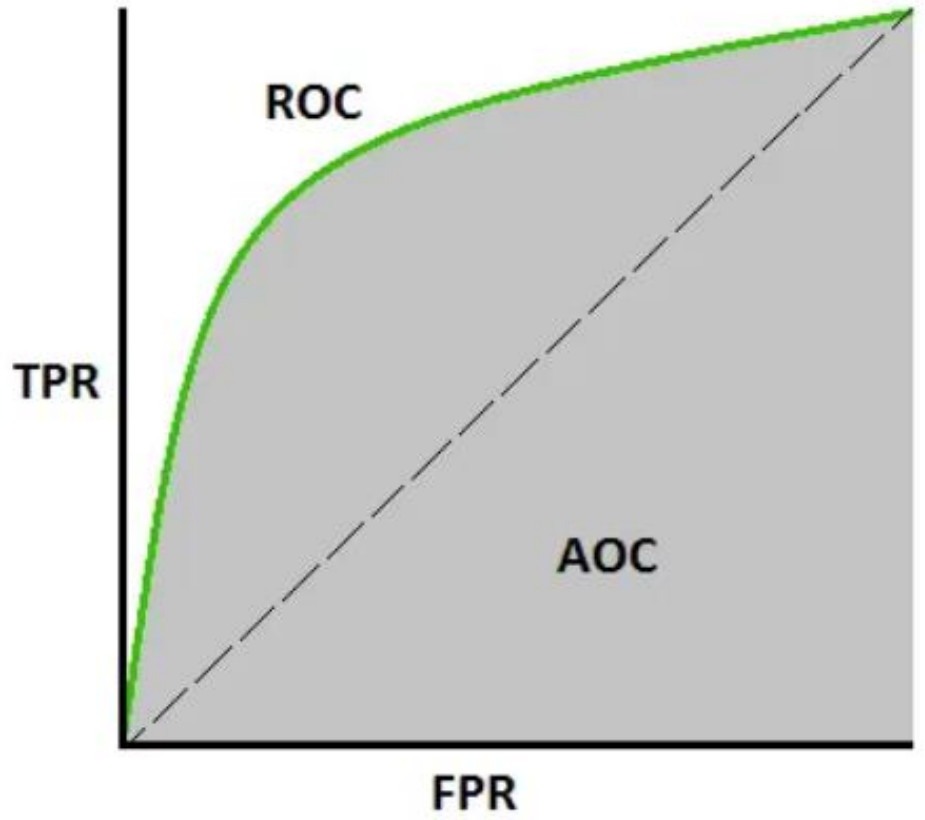

Confidence Interval

- Suppose I am interested in calculating the average age of IITJ students

- I randomly take 100 students and calculate the mean of their age. Say the mean is 20.5

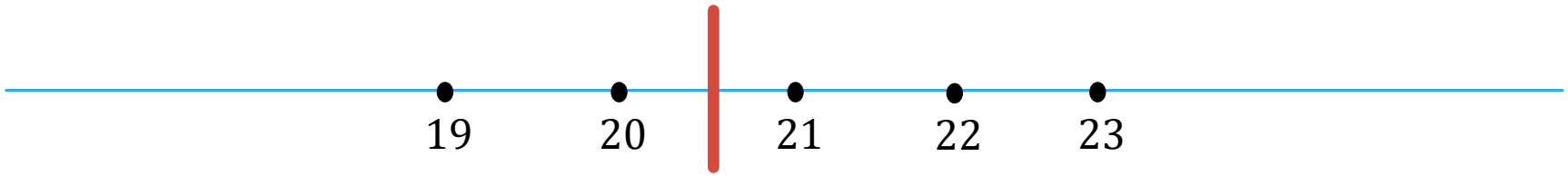

Confidence Interval

- Suppose I am interested in calculating the average age of IITJ students
- I randomly take 100 students and calculate the mean of their age. Say the mean is 20.5
- I repeat the above steps many times

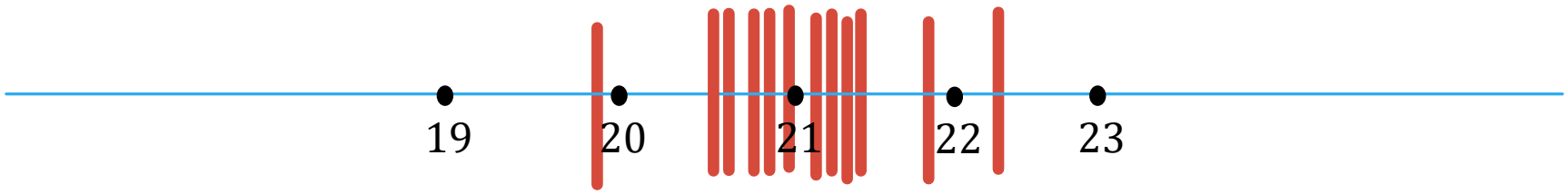

Confidence Interval

- If I want 95% confidence interval

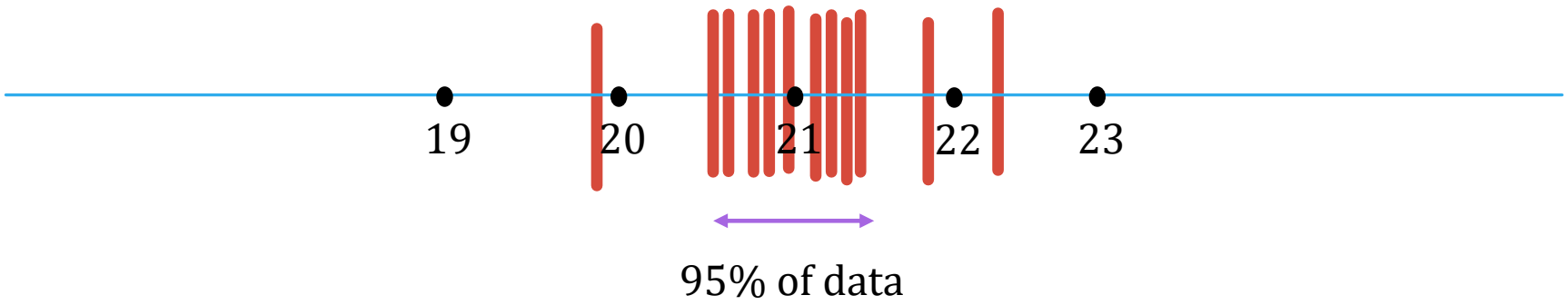

How to Find Confidence Interval

- Find out the mean of the measured data

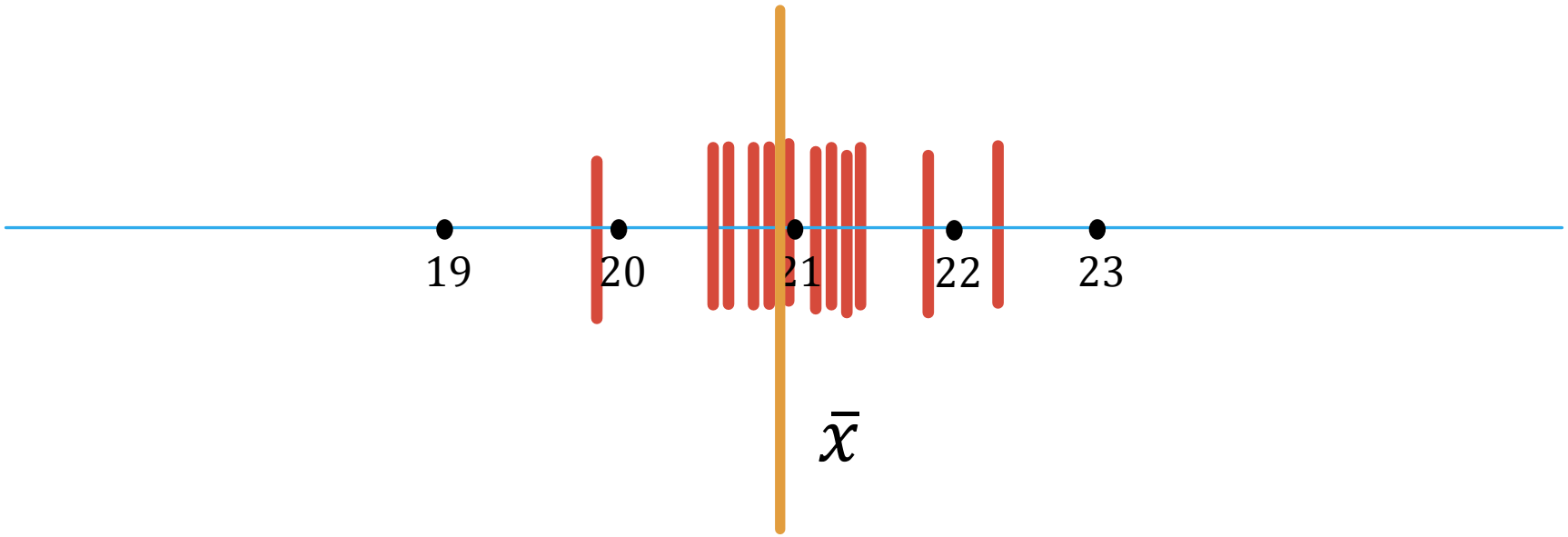

How to Find Confidence Interval

- Find out the mean and standard deviation of the measured data

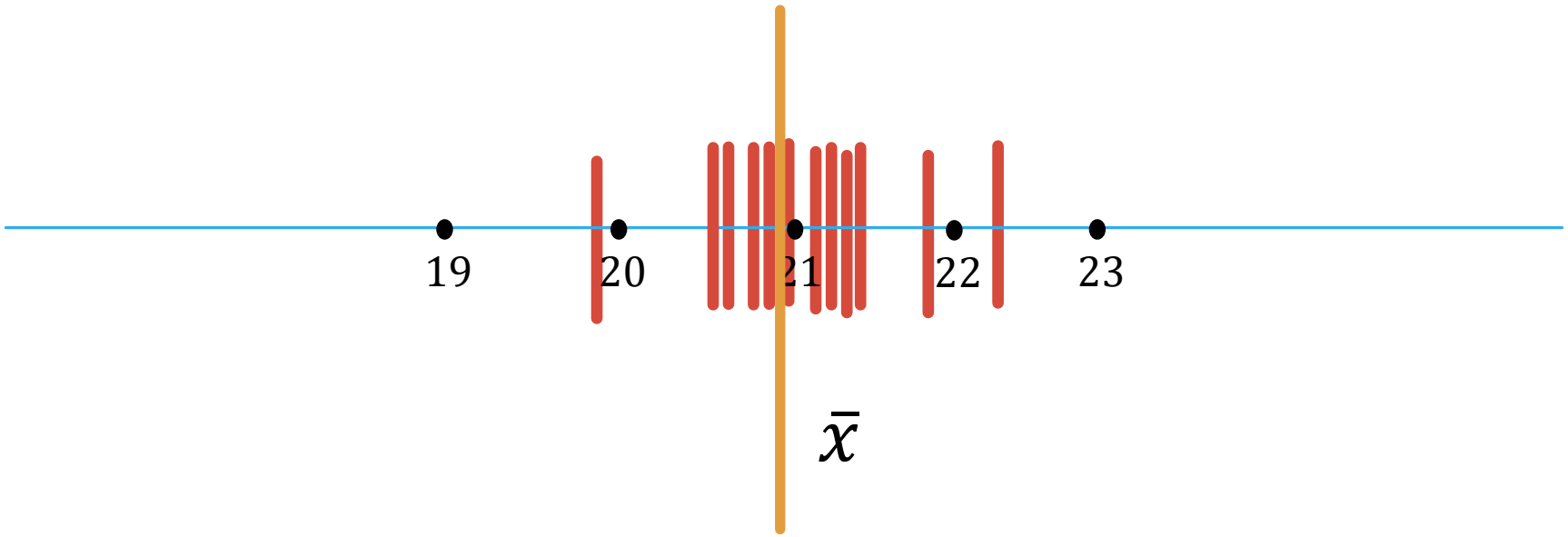

How to Find Confidence Interval

- Find out the mean and standard deviation of the measured data

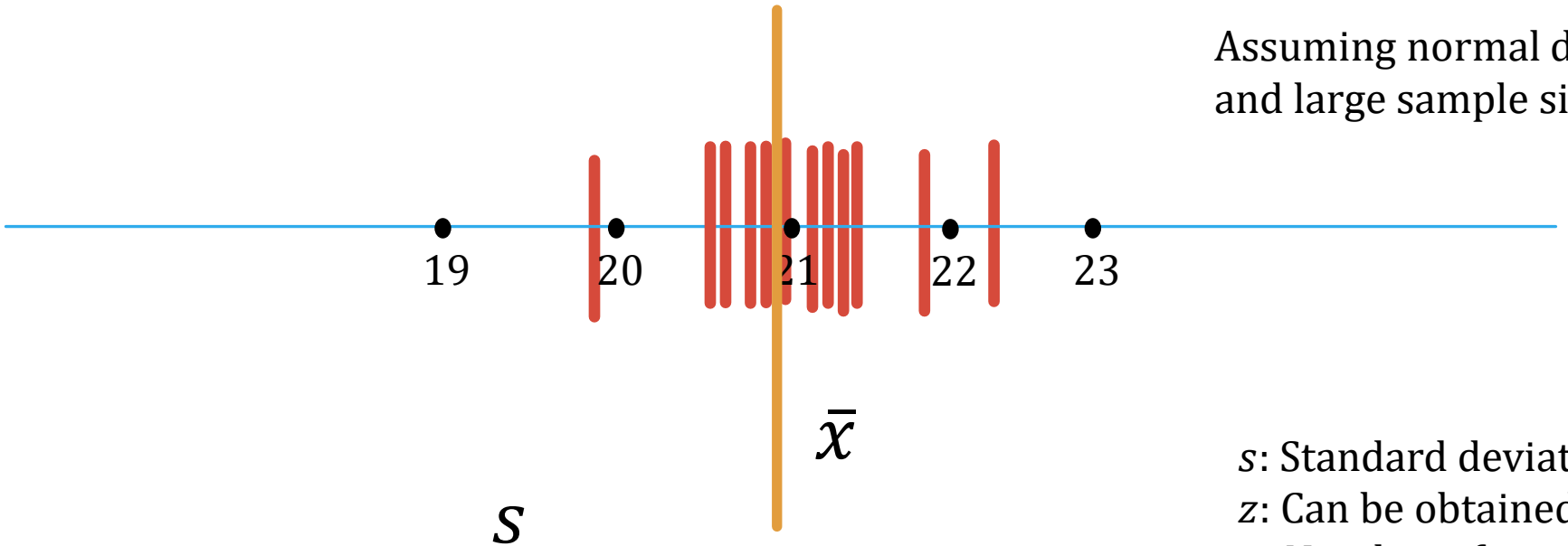

Assuming normal distribution and large sample size

$$CI = \bar{x} \pm z\frac{s}{\sqrt{n}}$$

s: Standard deviation
z: Can be obtained from a table
n: Number of samples

Confidence Interval

- If I want 95% confidence interval

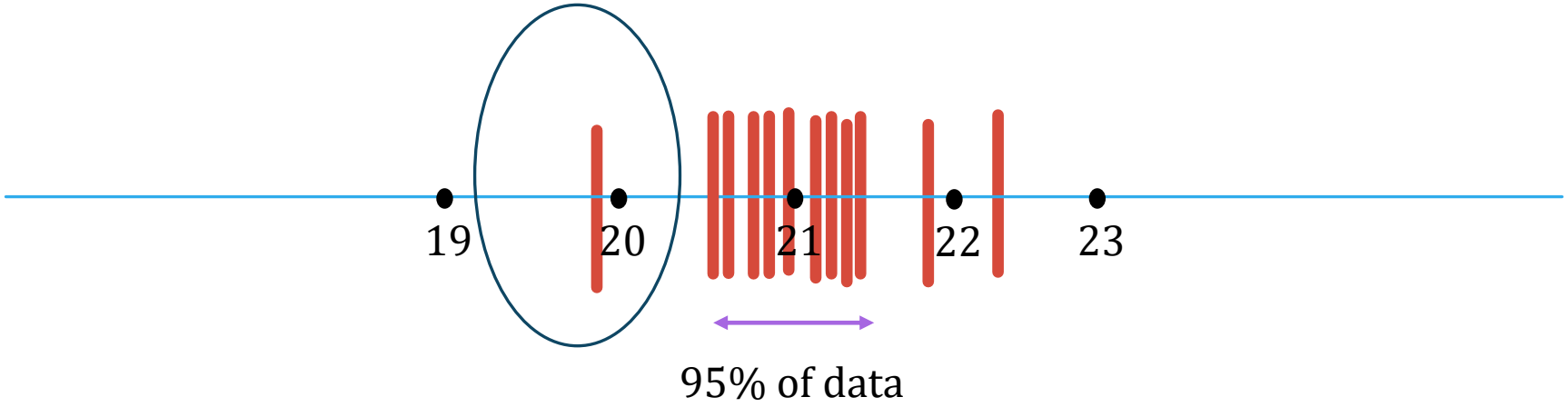

If a measurement lies outside the 95% confidence interval, we say $p < 0.05$, i.e., there is a statically significant difference between the true mean age and the highlighted mean age (if we consider the example of calculating mean age of students at IITJ)

How is Confidence Interval Relevant in MedIA?

- Suppose you perform benign vs malignant classification of histopathology images
- You have taken a large dataset and divided it randomly into 70% training, 10% validation and 20% test sets
- Get the test AUROC
- Repeat the above two steps with different random splits (say, 100 random splits)
- You get 100 AUROC values
- Now, from the 100 AUROC values, you randomly sample 30 and get the mean AUROC
- Repeat this process 50 times
- Now, you can calculate the CI for mean AUROC
- A tight CI shows stability of performance

Cell Image Analysis

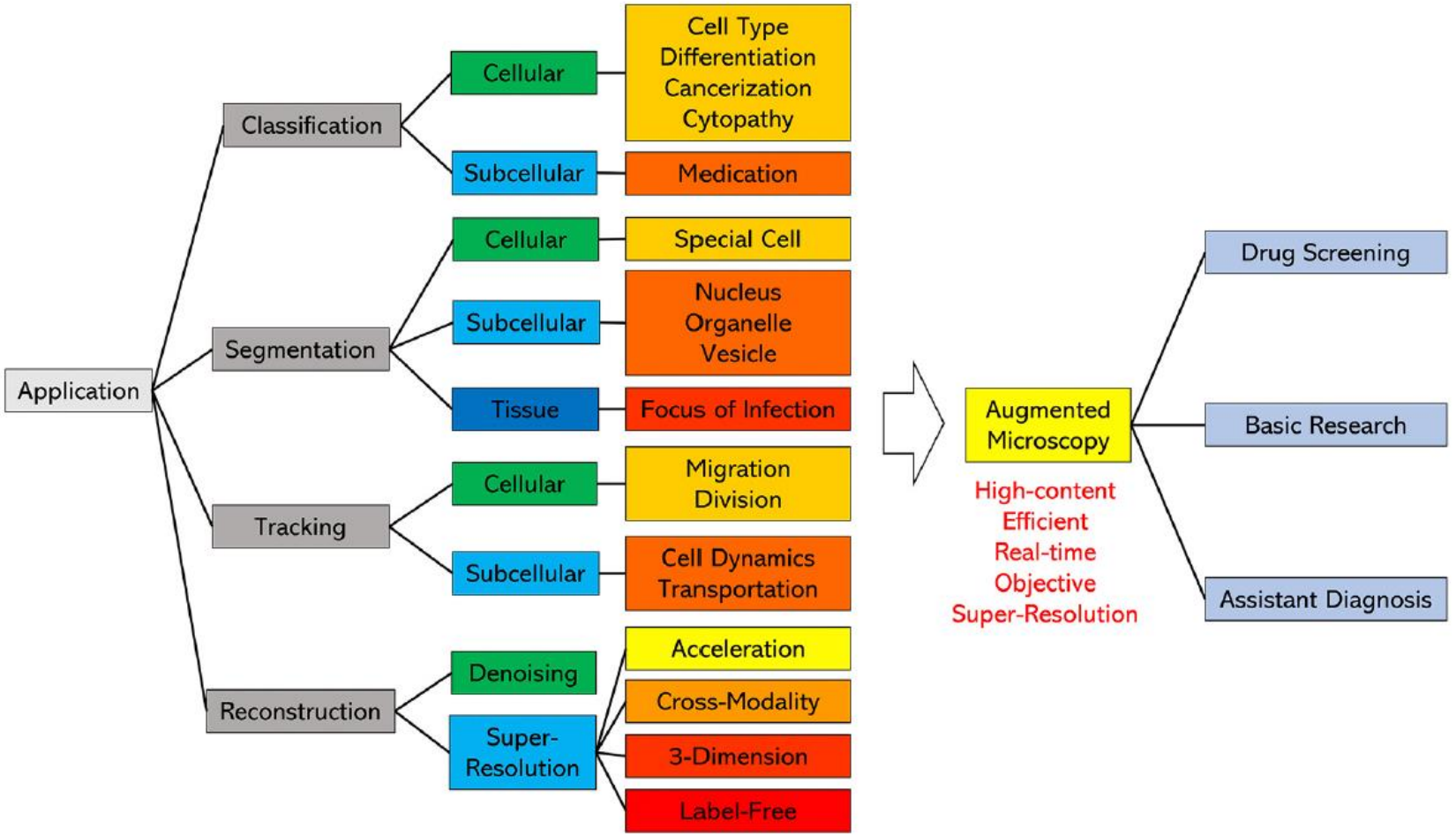

Cell Tracking based on Graph Matching

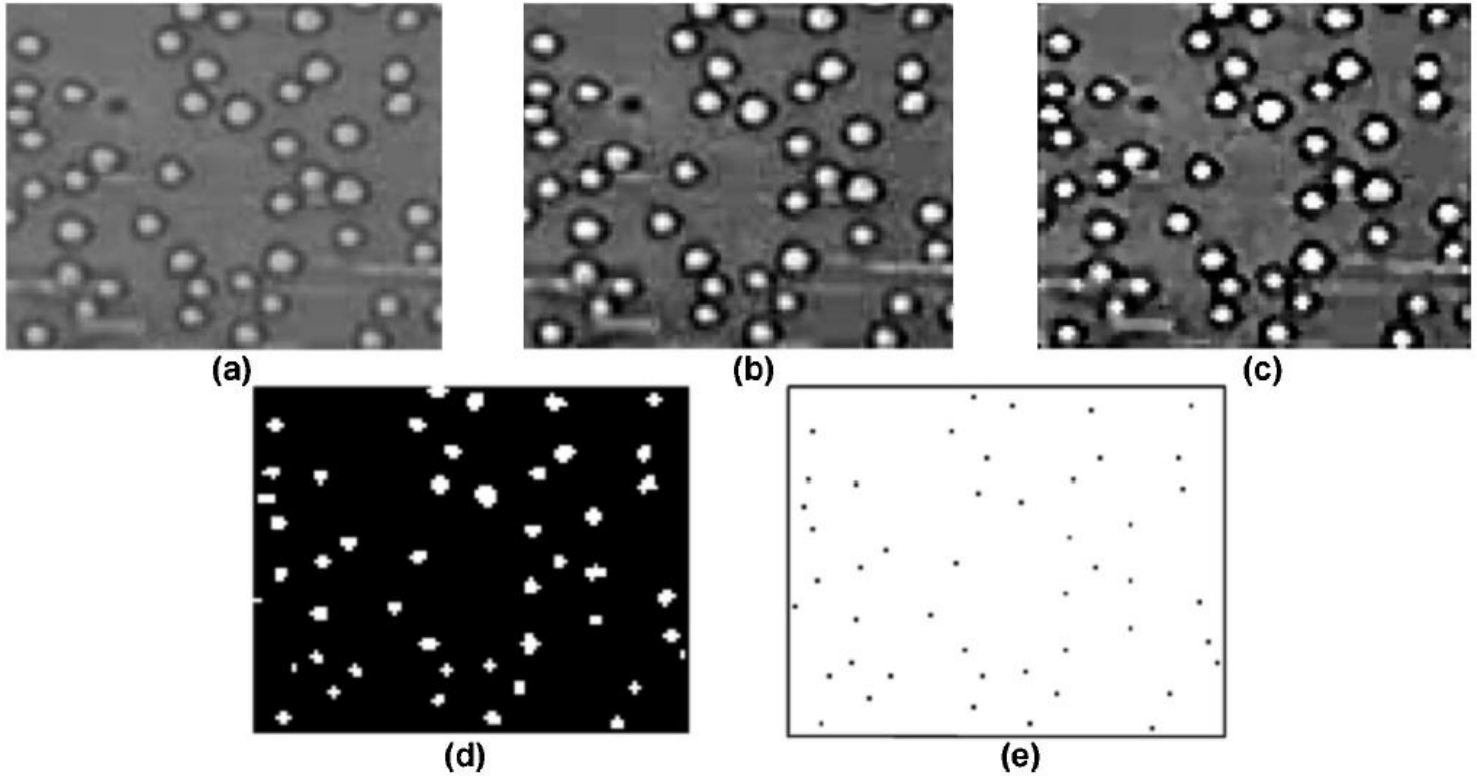

Fig. 4 – Image sequence going through the various pre-processing stages. (a) Original image sequence, (b) image sequence after contrast enhancement, (c) image sequence after median filtering, (d) image sequence after entropy thresholding, (e) image sequence after connected component labeling and centroid extraction.

Cell tracking in microscopic video using matching and linking of bipartite graphs

Cell Tracking based on Graph Matching

- Max entropy thresholding to segment the cells
- Maximum cardinality minimum weight bipartite matching

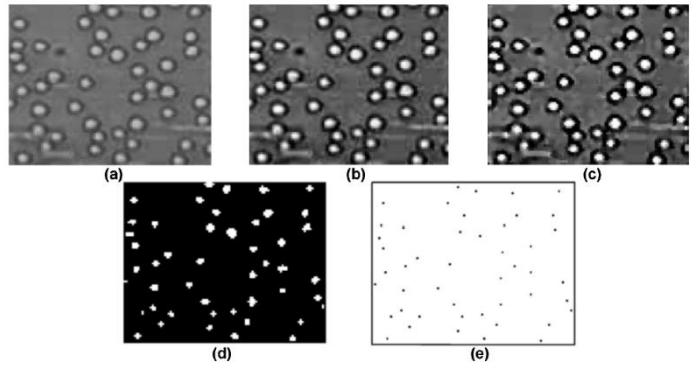

Fig. 4 – Image sequence going through the various pre-processing stages. (a) Original image sequence, (b) image sequence after contrast enhancement, (c) image sequence after median filtering, (d) image sequence after entropy thresholding, (e) image sequence after connected component labeling and centroid extraction.

Mean motion

$$\Delta x_{k,k+1} = \overline{x_{k+1,b}} - \overline{x_{k,a}}$$

$$\Delta y_{k,k+1} = \overline{y_{k+1,b}} - \overline{y_{k,a}}$$

Past motion

$$x\_\alpha_{k,i} = (x_{k,i} - x_{k-1,i}) + \lambda_2 * x\_\alpha_{k-1,i}$$

$$y\_\alpha_{k,i} = (y_{k,i} - y_{k-1,i}) + \lambda_2 * y\_\alpha_{k-1,i}$$

Updated location

$$x'_{k+1,i} = x_{k,i} + \lambda_1 \Delta x_{k,k+1} + \lambda_2 x\_\alpha_{k,i}$$

$$y'_{k+1,i} = y_{k,i} + \lambda_1 \Delta y_{k,k+1} + \lambda_2 y\_\alpha_{k,i}$$

Weight

$$w'_{i,j} = \sqrt{(x'_{k+1,i} - x_{k,j})^2 + (y'_{k+1,i} - y_{k,j})^2}$$

Cell Tracking based on Graph Matching

- Max cardinality min weight bipartite graph matching

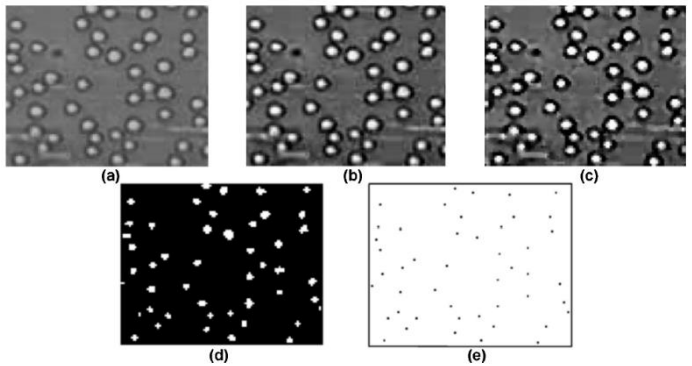

Fig. 4 – Image sequence going through the various pre-processing stages. (a) Original image sequence, (b) image sequence after contrast enhancement, (c) image sequence after median filtering, (d) image sequence after entropy thresholding, (e) image sequence after connected component labeling and centroid extraction.

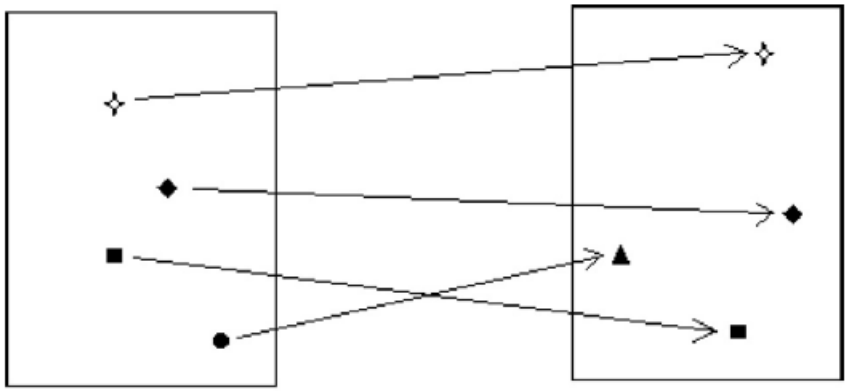

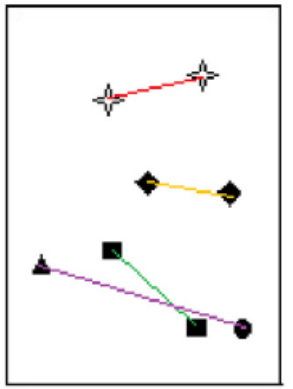

Fig. 1 – (a) Cells tracked over two consecutive frames F_k and F_{k+1}. Same shapes denote same cells and arrows denote matches. (b) Superimposition of the two frames into one frame to show the Euclidean distances between the matched cells.

Cell Tracking based on Graph Matching

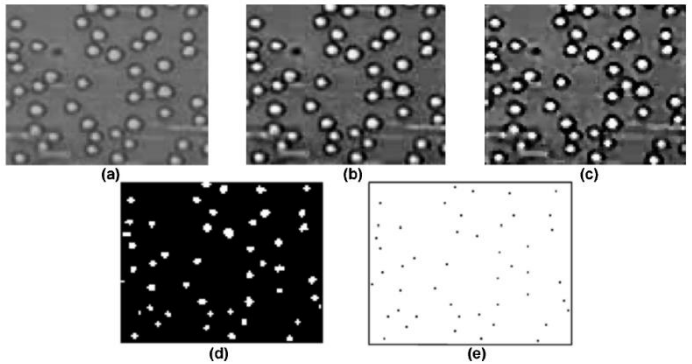

Fig. 4 – Image sequence going through the various pre-processing stages. (a) Original image sequence, (b) image sequence after contrast enhancement, (c) image sequence after median filtering, (d) image sequence after entropy thresholding, (e) image sequence after connected component labeling and centroid extraction.

- Max cardinality min weight bipartite grap matching